Detection and Optimization of Weak Photoelectric Signal in Intelligent Optical Film Deposition System

Shijun Xu[1], Xiaoling Ren[2], Chunmin Zhang[3]

[1]School of Science, Xi'an Technological University & Xi'an Jiaotong University, Xi'an 710032, China
[2]School of Computer, Xi'an Polytechnic University, Xi'an 710048, China
[3]School of Science, Xi'an Jiaotong University, Xi'an 710049, China
xushijun000@sina.com

Abstract - For the thin-film thickness monitoring(TFTM) system, a new technology based on a double-frequency modulation equipment, a photoelectric four-light path system, a comprehensive digital processing-controlling system and a dual-lock-phase circuit system, has been successfully developed by optimizing the circuitry and data processing to improve the precision of the photoelectricity-extremum technology. The novel technique includes analog circuits of multi-stage amplifier, symmetrical dual-lock-phase amplifier, anti-disturbance circuit technique, digital division, anti-pulse-disturbance digital filter, linearization of digital display, removal singular data, and extremum judgment with ΔR algorithm. Experiments show that the detection and optimization methods on weak photoelectric signal take advantages of higher stability and better static and dynamic precision in controlling the thin-film thickness. The static drift ratios of two output electric signals are equal to or less than 7%/h, as well as the analog signal-to-noise ratios of reference or measurement paths are more than 500. The digital display sensitivity responding to reflectivity is higher, the linear regression factor of the digital display data is 0.979, and the display resolution of low reflectivity is equal to 0.02%. Compared with the conventional TFTM system, the uncertainty of monitoring signal in the new technology declines one order of magnitude, consequently, the drift ratio of monitoring signal is approximately equal to 0.

Index Terms - Optical Detection, Signal Optimization, Compound Filteration, Film, Four-light Beams.

1. Introduction

The principles of optical thin-film thickness monitoring (TFTM) include the photoelectricity-extremum method (PEEM), the wide spectrum monitoring method, the quartz crystal oscillation method, the ellipsometry measurement method, etc.[1-4]. Among these techniques, the PEEM is widely used. In order to achieve exact, stable, and automatic monitoring via the PEEM, the weak photoelectric detection signal must be processed with high precision. The conventional TFTM system[5] utilizes monochromatic light modulation, a single analog circuit filter processing, and digital display. Moreover, the corresponding judgment and operation are performed manually or mechanically. The anti-disturbance abilities and stabilities of the light source, photomultiplier tube, and their power supplies are highly demanded by the conventional TFTM system. The aseismatic performance and stray light suppression ability of the conventional TFTM system are relatively weak. The photoelectric monitoring signal is only processed byanalog filtering, the stability and accuracy of photoelectric monitoring signal are relatively low, and thereby this affect the operation of the switch baffle and the development of automatic film deposition system[5]. Recently, the data acquisition and filter system have been added to the conventional TFTM system[6], and therefore, some of the noises and random errors have been inhibited.

In the reference[7], the principle of a PEEM TFTM system has been suggested based on the four-light beams and dual-frequency modulation, which makes the significant improvements of the stability and accuracy of the monitoring signal possible. However, to achieve the high stability and accuracy for the monitoring signal and the development of automatic thin-film deposition system are depended on the signal processing by the analog circuits, the data acquisition, the digital processing, and the control quality. In this work, a multiple optimized scheme involving the analog circuits of multi-stage amplifier, symmetrical dual-lock-phase amplifier, anti-disturbance-circuit technique, digital division, filters shielded from digital pulse disturbance, linearization of digital display, singular data removal, and extremum judgment with ΔR algorithm has been proposed based on four-light-beam TFTM. The experiments are satisfactory.

2. Signal Characters Of The Thin-Film Deposition ystem

In the thin-film deposition system with four-light beam, the light emitted from a light source will be split, and then modulated with dual-frequency, respectively. Through two silicon photo cells, the phase-lock demodulation signals of the reference and test circuits are obtained, and at the same time, the reference and test light beams are also obtained. The test light-beam with the information of the thickness of the thin-film and reference light-beam are transmitted and converted by the same optical fiber, monochromator and photomultiplier tube. The superposition of the reference signal and test signal is separated through the amplifier and lock-phase circuits, and then, they are acquired by the data acquisition card. At last, the whole functions of controlling of the thin-film thickness are realized with the methods of high precision digital processing and the program controlling.

The TFTM signal outputed by the photodetector are the 33Hz test channel and 383Hz reference channel demodulated signals outputed by two silicon photo cells, 33Hz test signal outputed by the photomultiplier tube which contains the thin-

film thickness information and the uncertain information of the optical system, and the 383Hz reference signal which contains only the uncertain information of the optical system. With the DC6V30W light source, the demodulated signal of the 33Hz test channel is approximate to a square wave signal, the output impedance is approximate to be 20Ω, and its low electrical level has an obvious disturbance of the 383Hz signal (square wave U_{PP}≈350mV, disturbanceU_{PP}≈10mV). The 383Hz demodulated signal of the reference channel is similar to pulse signal with output impedance about 20Ω and 33Hz disturbance (pulse U_{PP}≈200mV, disturbance U_{PP}≈20mV). The test signal and reference signal output impedance of the photomultiplier tube is about 3MΩ (test signal U_{PP}≈8mV, reference signal U_{PP}≈0.6mV), and the high-frequency disturbance (KHz) and low-frequency disturbance (1Hz) are also included.

3. Optimization Scheme to Weak Singal

Based on the four-light-beam, dual-frequency modulation of the PEEM, the weak signal output of the photoelectric sensor is handled multiply (see Fig. 1). The signal first passes through the multi-stage amplifier circuit, and then, it is detected by a symmetrical dual-lock-phase amplifier (on the left dashed box of the Fig. 1) with high precision. At last, the reference and test signals are processed and controlled by the computer after data acquisition. The right side of the dashed box represents the digital processing and controlling analysis system. The smoothing of the scanning data is handled after the monitoring of the thin-film deposition, and other processing and controlling are handled in real time.

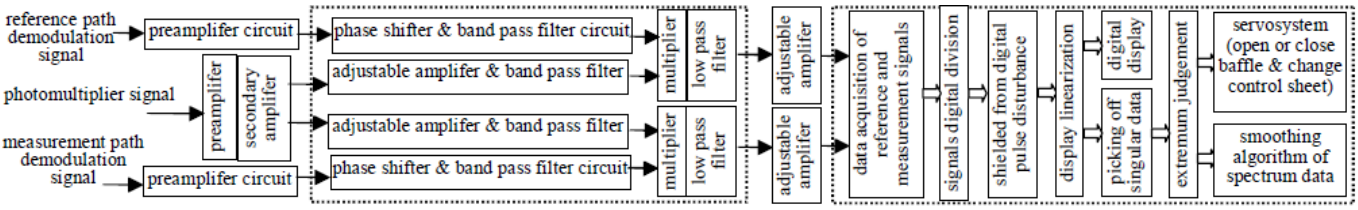

Fig.1. Flow chart of the optimum signal processing.

3.1. Multi-stage Matching Amplifier Circuit

The maximum power transmission can achieved through the matching of the input impedance of the preamplifier and the output impedance of the photodetector, and the maximum signal to noise ratio of the output can be obtained when the amplifier is operated in the best source resistance state. The GDB-240 type 11-level photomultiplier tube with high output impedance (3MΩ) is used in this study, however, the internal resistance of the 2CR series silicon photocell is very low (about 20Ω), and thus, the preamplifiers for the signal and demodulation are different.

Field-effect transistor is a voltage-controlled device with high input impedance, low noise, and strong anti-radiation. The 3DJ7 series N-channel junction field-effect transistor is selected to construct the preamplifier circuit of the photomultiplier tube[5]. At first, the input and output impedance are matched through the negative feedback, and then, the gain, bandwidth, and noise are checked.

The conventional proportional amplifier is used for the preamplifier circuits of the two demodulated signal output of the silicon photo cell[8]. Otherwise, the secondary and three-stage-adjustable-gain amplification can be achieved with the conventional proportional amplifier.

3.2. Symmetrical Dual-lock-phase Amplifier Circuit

Lock-phase amplification possesses phase sensitive detection to alternating signal. By multiplying the measured and demodulated signals with the same frequency and phase-lock relationship, the responses are only obtained for the measured signal and noise signal which has the same frequency, multiplication, or the same phase with the demodulated signal. Thus the detection sensitivity can be greatly improved and the noise can be suppressed (the equivalent noise bandwidth10^{-3}-4×10^{-4}Hz, the gain up to 220dB). The AC input is amplified to be DC output, which is effective for weak signal detection.

The test signal containing film thickness information and uncertain information from the optical system is detected with a single lock-phase. Therefore, the inherent disturbance uncertainty of the optical system can not be eliminated, and the nonlinear disturbance and thermal noise of the circuit system will be imported. In this study, in addition to the 33Hz test signal and the corresponding demodulated signal, the 383Hz reference signal with the uncertain information of the optical system and the corresponding demodulated signal are introduced. We propose symmetrical reference channel cross-correlation detection circuit and test channel cross-correlation detection circuit, and the corresponding core is phaser, multiplier, and filter.

Before phase-lock, the mixed signal of 33Hz & 383Hz must be possessed by the frequency division filter. In order to improve the S/N and make the passband of the bandpass filter better, two three-level associated second-order phase-lock bandpass filters with symmetrical structures and devices are utilized. The phaser (Fig.2) is a RC circuit associated with a non-inverting terminal of a operational amplifier. The phase shift φ is controlled by a variable resistor. When R_F=R_f, $\varphi(\omega)$=2tan^{-1}(ω/R_tC_t). Switching analog multiplier[7] uses the 3DJ7H type field-effect transistor as the analog switch. The DC output is proportional to the input signal, and the positive and negative polarities correspond to the in-phase and out-phase.

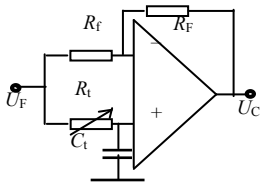

Fig.2. Phaser circuit.

3.3. Anti-disturbance Electronic System

Systematical anti-disturbance techniques are listed as follows. Four channels of the lock-phase circuit are arranged parallel and symmetrically to reduce the disturbance; lock-phase circuit and amplifier circuit are arranged individually (each belongs to a individual circuit board) to avoid the disturbance of post-amplifier imposing on the pre-amplifier; metal film resistors with small electrical noise and high-performance shielded signal line are selected; the power cord is widened, and the direction of ground wire is arranged consistently with the direction of data transmission; the specific power is encapsulated with a metal shielding box and placed on the opposite side of the lock-phase and amplifier circuits in order to avoid the electrical disturbance between these devices and to facilitate heat dissipation; under low frequency, the ground connection of data acquisition system is guaranteed by paralleling coarse ground wire to a point (the grounds of the data acquisition card, circuit board, and power supply are connected with the same wire) to inhibit the impedance noise of the common ground wires and avoid the coupling of digital signal to analog signal.

3.4. Digital Division & Anti-pulse Disturbance Filter

Two signals outputed by the circuit system were acquired via the data acquisition card PCL818. These two signals contain high-frequency disturbance, pulse disturbance, and low-frequency disturbance. The disturbances include differential mode and common mode components. These two signals contain common stable factors of the light source, photomultiplier tube and its power, optical fiber, monochromator, and circuit. The disturbance amplitudes and the phases of these two signals are almost identical, and only the amplitudes are different. To achieve high-precision and high stability monitoring, digital division and filters shielded from digital pulse disturbance must be carried out.

3.4.1. Digital Division Operation

This digital division operation is a necessity for the four-light beams and the dual-frequence modulation in the PEEM TFTM. Moreover, the digital division operation is the key component of the digital processing system. Because the test and reference signals share the light source, photoelectric sensor, circuit, and acquisition card, the common-mode high-frequency disturbance and common-mode low-frequency drift. Thus the disturbance can be eliminated furthest by using the "test÷reference" operation. Otherwise, compared with analog circuit divider, the digital division operation does not need hardware, and it is simple, reliable and highly precise.

3.4.2. Anti-pulse Disturbance Digital Composite Filters

Anti-pulse disturbance digital filtering method is a composite of the average method and median method under the normal circumstance of $3 \le n \le 14$. In this study, filter shielded from digital pulse disturbance method is used, and n=24 (24 continuous samplings) with removing the two maximum numbers and two minimum numbers. Two original n=12 algorithms are merged. The rotating stability of the modulation high-power gear motor and the machining precision of the modulation plate will introduce common-mode low frequency disturbance, the motor speed is 500rel/min, and the data sampling frequency is 100Hz, i.e., the modulation plate circling round corresponds to the sampling number of (100÷500)×60=12. There is always a large number and a small number in the debugging process. Considering the cycles of the thin-film deposition signal (10s~800s), in order to enhance the filtering effect, the corrective algorithm (plate modulation circling around twice with 0.24s corresponds to a number of digital display) is taken. This will not only suppress the high frequency disturbance and pulse disturbance, but also eliminate the common-mode low-frequency disturbance introduced by the modulation system.

3.4.3. Optimization of Digital Division and Anti-pulse Disturbance Algorithm

As analyzed in section 3.4.1, the division operation of "test÷reference" can maximally eliminate the common-mode disturbance and drift. However, whether the orderly combination of the division operation and the algorithm shielded from digital pulse disturbance can effectively suppress the common-mode disturbance or not is a key problem. The disturbance amplitudes and phases of the test and reference signals are almost the same, while the pair of test and reference signals obtained by the multi-channel scanning of the data acquisition card has phase delay corresponding to 1%s. If the digital division operation is before the algorithm shielded from digital pulse disturbance, the phase inconsistency of the divided data is only the small phase delay corresponding to the 1%s time delay. If the algorithm shielded from digital pulse disturbance is before the digital division operation, the phase inconsistency of the divided data will be the phase delay corresponding to the 24%s time delay. As a result, the suppression effect of the common-mode disturbance will be reduced, and even the four-light beams and dual-lock-phase amplifier circuit which are designed to eliminate the common-mode disturbance of the system turns to be meaningless. In this study, the digital division operation is before the algorithm shielded from digital pulse disturbance.

3.5. Linearization of Digital Display

Due to the nonlinear effect of the photoelectric conversion in the photomultiplier tube, and filtering, amplification, and lock-phase in circuit, the data after division and digital filter are non-linear with the film reflectivity. The linearization of

digital display, i.e., physical explanation (calibration) is needed. The process is summarized as follows. A series of standard films with known reflectivity (reflectivity from 0.04% to 96%) are tested, and the corresponding display numbers are obtained. And then, the quadratic polynomial fitting is used, the fitting function is taken as the display linear function before the "display".

20 groups of data are tested, and the quadratic polynomial fitting function for $\hat{R} = \hat{\beta}_0 + \hat{\beta}_1 S + \hat{\beta}_2 S^2$ based on the least square method is

$$R=0.0256+0.2670S+0.0610S^2 \quad (1)$$

where R is the reflectivity, while S and R are the corresponding display number.

3.6. Singular Data Removal and Extremum Judgment

In the PEEM, accurate judgment to extreme point is a key step. Because the changes of the reflectivity data in the vicinity of extreme point is very small, but coarse value(once about 5s) will emerge after the linearization of digital display. The coarse value will affect the successful judgment to extreme point. Therefore, extremum judgment and singular data removal should be combined.

The thought of the singular data removal is listed as follows. For any continuous displayed three data N_1, N_2, and N_3, we define $\varepsilon_1=N_2-N_1$, $\varepsilon_2=N_3-N_2$. Under the condition of very high sampling frequency, $\varepsilon_1\approx\varepsilon_2\approx\varepsilon$ is tenable. According to the changes of the actual transmissivity and reflectivity of the thin-film, the range of N_3 is $N_3\in(N_2-\varepsilon,N_2+\varepsilon)$. Therefore, N_3 can be deemed to be normal when $N_3\geq N_2\geq N_1$ and $N_3\leq N_3'=N_2+k\varepsilon$. Otherwise, N_3 should be deemed as singular data, and be replaced with N_3'. Under other circumstances of N_1, N_2, and N_3, the operation can be deduced analogously, in which $|k|$ is selected as a value around 1 according to the experiment.

After the singular data have been removed, the extremum can be judged with a simple and practical ΔR algorithm. Based on the precision requirement for monitoring, a positive and negative change tolerance δ is prior to be set for the reflectivity R. According to the features of the data nearby the extremum point, the extremum point is obtained as the positive and negative change of the reflectivity ΔR is consistent with $|\Delta R|\geq\delta$. This method obviously need small disturbance of the signal and higher requirement for the pre-stage digital filter, or else, ΔR will change to be positive and negative ceaselessly, which will results in the misjudgment of the extremum point. The design of the four-light beams, multi-stage digital filter, and data processing model provide a guarantee for the stability of the signal.

3.7. Smoothing of the Scanning Spectral Data

In order to obtain the spectral characteristics of film, the spectral scan is carried out after the end of the TFTM. The spectra can be drawn after smoothing of the scanning data. Because the data processing is not in real time, the scanning data can be smoothed using the five-point cubic spline algorithm[9] with expensive computational cost.

The practical five-point cubic spline algorithm is used to eliminate the rough data caused by the random high-frequency disturbance, and its essence is the data low-pass filter. According to the principle of least square, the filtering factor of y_i is (-0.0857,0.3429,0.4857,0.3429, -0.0857) obtained from $2N+1$ set of data (t_i, y_i), and using this filtering factor is reasonable.

4. Test and Analysis

The composite processing technology of the weak signal in photoelectric detection in the TFTM is performed in the static characteristic test and the thin-film deposition monitoring, including the electric system test, digital display test, and film deposition monitoring test.

4.1. Tests of the Dual-lock-phase Amplifier Circuit and Anti-disturbance Electronic System

With isolating the digital circuit, the signal to noise ratios of the test outputs and reference outputs are 800 and 500 after the completion of debugging of the analog circuit system. The output voltages are about 0.7V and 0~2.8V, respectively. The static drift rates of these two signals are within the scope of ≤7%/h, which are near to the requirements of the digital acquisition and processing system (two-channel signal output voltages are within ±5V, the signal to noise ratio are in the scope of≥300, and the static drifts are in the scope of≤10%/h). The outputs of the test and reference channels contain high frequency (kHz), low frequency (less than 1Hz), and pulse disturbance. The disturbance includes differential mode and common mode components, the common mode component refers to those that the two signals contain common stability information of the light source, photomultiplier tube and its power, optical fiber, monochromator, and circuit system. The disturbance amplitudes and phases of the test and reference signals are almost the same. These characteristic signals facilitate the subsequent digital processing, and all kinds of disturbances and instability factors can be easily eliminated to the best.

4.2. Character of the Digital Display

4.2.1. Sensitivity of the Reflectivity Response

Through differentiating for Eq.(1), one will obtain

$$\mathrm{d}S/\mathrm{d}R=1/(0.267+0.122S) \quad (2)$$

The larger dS/dR means that the response of the circuit and display system to the changes of the reflectivity is more sensitive.

When R=100%, one will obtain $(\mathrm{d}S/\mathrm{d}R)_{\min}=1.799>1$ from Eq.(1) and Eq.(2). Therefore, the response of the circuit and display system to the changes of the reflectivity is relatively large at the entire reflectivity range before the linearization of digital display. The response will be larger as the reflectivity is lower. If we take 60% of the $(\mathrm{d}S/\mathrm{d}R)_{\max}=(\mathrm{d}S/\mathrm{d}R)_{S=0}=3.745$ as the experience criterion for the judgment of the sensitivity level, the R=54.5%, i.e., $R\leq54.5\%$ is the high sensitivity range for this system from Eq.(1) and Eq.(2).

4.2.2. Linearization of Digital Display and Resolution

After performing linearization of digital display with Eq.(1), new 10 sets of test data will be obtained with display measurements of standard reflectivity values, and then linear regression is carried out. The calculated digital display linear regression coefficient is 0.9789≈1, and the correlation coefficient is r=0.9994 for the correlation coefficient test method. With respect to those the linear regression coefficient is almost equal to 1, the uncertainty in the test experiment, the stability of the digital display, and the measurement accuracy of the optical spectrum analyzer, the linearization of digital display mentioned above is apparently successful. The comparison between the correlation coefficient r and the critical value of $r_{0.01}(10)$=0.7080 shows that the linearity of the digital display is very high, and the remaining deviation is very small, which means that the system has photometric function to some extent.

ΔS_{min} is defined as the lowest static range of the digital tube (caused by film reflectivity), and then, $\Delta R_{min}=(dR/dS)\Delta S_{min}$ represents the resolved minimum change of the reflectivity, i.e., the resolution limit of the digital display. After test, the resolution limit for high-reflectivity film of digital display is ΔR_{min}=0.12%, while the resolution limit for the low-reflectivity film case is ΔR_{min}=0.02%. These resolution limits meet the requirements of the high-precision TFTM.

4.3. Test Result

An overall test has been performed for the combined processing of the photoelectric detection signal in the TFTM. The static characteristic is tested in the warm-up phase before the open of the baffle. A large number of static test data for the double-side polishing K9 flat glass (R=8.12%) are analyzed using the linear fitting drift coefficient β, the sum of the squared standard deviation S_T, the standard deviation of the linear regression U_A, and the dispersed degree of the linear regression s. The results are shown in Tab. 1. Where "A" row is the data analyses of the test signals, the equivalent data obtained from a single light beam, a single lock-phase the common system, and plus with the digital filter processing and digital display data after the linearization. "B" row is the data analyses of a "test÷reference" division operation, and without the filter shielded from digital pulse disturbance algorithm and linearization of digital display. "C" row is the data analyses with the linearization of digital display and the filter shielded from digital pulse disturbance algorithm before the division operation. "D" row is the data analyses with the linearization of digital display and the division operation before the filter shielded from digital pulse disturbance algorithm.

By comparative analysis of Table.1, we can conclude that the data in the "B" row illustrate that the division algorithm significantly restrains the common-mode disturbance, improve the static stability, slightly inhibit the drift (known by the β index). Deduced from the U_A+s, the final monitoring signal linearity has been greatly improved by the linearization of digital display, filters shielded from digital pulse disturbance, and digital division. The uncertainty of the signal has been greatly reduced, and the drift rate is close to 0. The data analyses of the "C" and "D" rows indicate that the design of the division operation before the filter shielded from digital pulse disturbance algorithm is more reasonable.

Table.1. Analysis of static test data.

rows	β	S_T	U_A+s
A	-0.00004126	0.00040064	0.00599
B	0.00003680	0.00008826	0.00255
C	0.00000796	0.00000321	0.00048
D	-0.00000442	0.00000205	0.00032

In the ZnS and MgF_2 TFTM, based on the reasonable static stability and sensitivity, the standard deviation of the thickness control is 0.50%, which is less than the common single-lock-phase system(1.25%). The results indicate that the design of the electric system, digital processing system, singular data removal, and extremum judgment with ΔR algorithm is reasonable.

5. Conclusions

The signal to noise ratios of the test and reference outputs are 800 and 500, and the output voltages are about 0.7V and 0~2.8V, respectively. The static drift rates of these two signals are within the scope of ≤7%/h, the disturbance amplitudes and phases of the test and reference signals are identical to each other, and the signals facilitate to be reprocessed digitally. For the digital display, the response of the circuit and display system to the changes of the reflectivity is relatively large at the entire reflectivity range, the response will be larger as the reflectivity is lower, the linearity of the digital display value is very high, the remaining deviation is very small, and the display resolution of low reflectivity is equal to 0.02%. The experiments show that the technique involving the symmetrical dual-lock-phase amplifier circuit design, the division operation before the filter shielded from digital pulse disturbance algorithm, the linearization of digital display, singular data removal, and extremum judgment with ΔR algorithm, ensures that the monitoring signal has a very small uncertainty (reduced by at least an order of magnitude) and the drift rate approaches 0. The experiments show that the high accurate and stabile detection for the weak signal will greatly improve the static, dynamic stability, controlling accuracy and automatic level of the TFTM.

References and Notes

[1] H. A. Macleod, Appl.Opt. 20, 1(1981).
[2] K. Tami and Y. Kiyoshi, Appl.Opt. 49, 34(2010).
[3] H. A. Macleod, Thin Film Optical Filters: 3rd ed, Institute of Physics Pub, Philadelphia(2001).
[4] G. Z. Sauerbrey, Z.Phys. 155, 1(1959).
[5] S. Xu, The Development of Real-time Monitoring System of Optical Thin-film Thickness, Dissertation of XAIT, Xi'an(2002).
[6] X. Y. Liu, G. Z. Huang and J. R. Yu, Chinese Journal of Vacuum Science and Technology 29, 4(2009).
[7] S. Xu, Journal of China Ordnance Society 7, 1(2011).
[8] Y. Li, Electronic Circuit on Detection, NWPU Pub, Xi'an(2006).
[9] M. Ma and C. Zhou, Data Collection and Processing Technology, Xi'an Jiaotong University Press, Xi'an(2008).